Electronic Supplementary Material (ESI) for Journal of Materials Chemistry A.

Electronic Supplementary Information

Nickel-cobalt oxide nanoparticles as superior electrocatalysts for enhanced coupling hydrogen evolution and selective ethanol oxidation reaction

Yong Zhang,[ab] Rong Liu,[ac*] Yi Ma,[ab] Ning Jian,[ab] Huiyan Pan,[d] Yongliang Liu,[ab] Jie Deng,[b] Luming Li,[b] Quan Shao,[ab] Canhuang Li,[e] Junshan Li[ab]*

a School of Mechanical Engineering, Chengdu University, Chengdu, 610106, China.

b Institute for Advanced Study, Chengdu University, Chengdu 610106, China.

c School of Preclinical Medicine, Chengdu University, Chengdu610106, China

d School of Biological and Chemical Engineering, Nanyang Institute of Science and Technology, Nanyang, 473004, China

e Catalonia Institute for Energy Research—IREC, Sant Adrià de Besòs, 08930 Barcelona, Spain

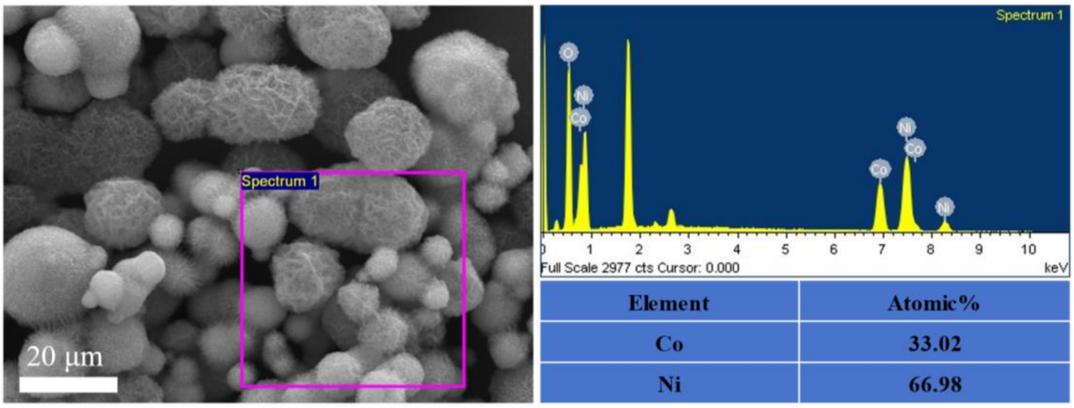

Element	Atomic%
Co	33.02
Ni	66.98

Fig. S1. The SEM-EDS spectra of $Ni_{0.67}Co_{0.33}O_x$.

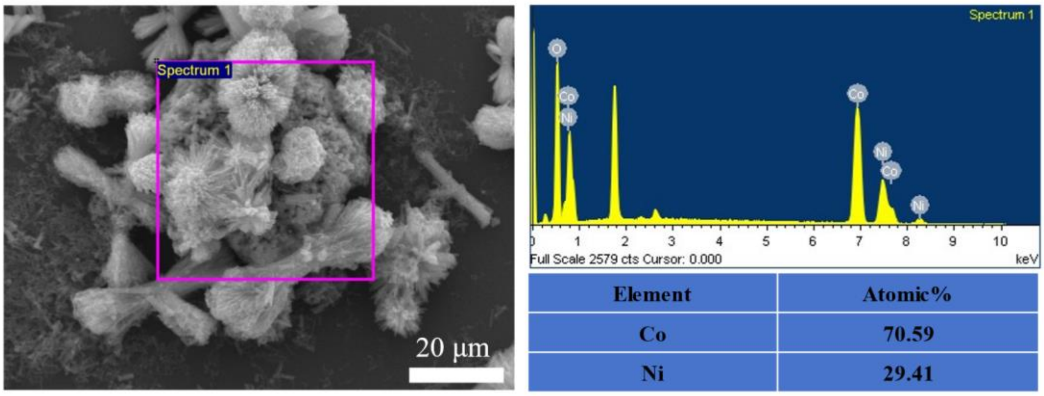

Element	Atomic%
Co	70.59
Ni	29.41

Fig. S2. SEM-EDS spectra of $Ni_{0.33}Co_{0.67}O_x$.

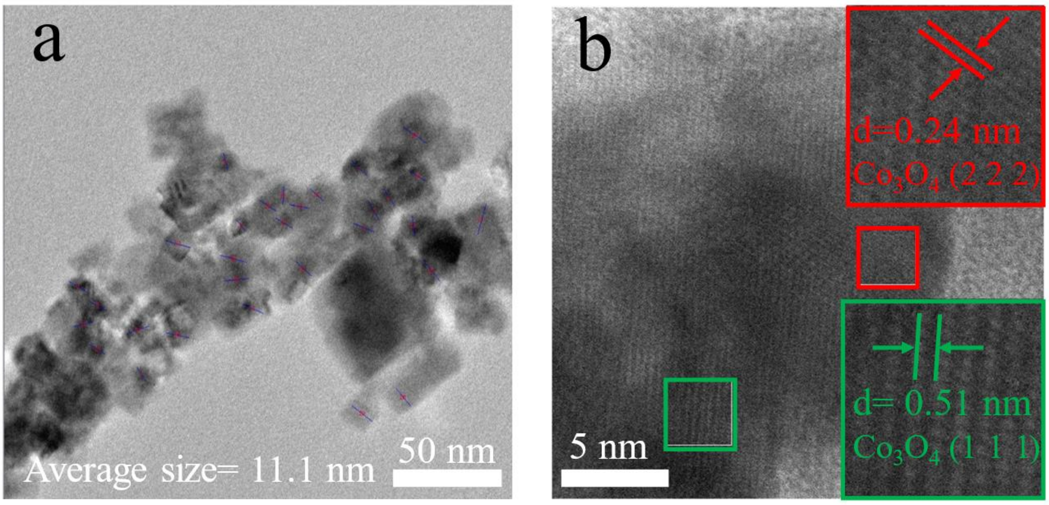

Fig. S3. a) TEM image and b) HRTEM image of $Ni_{0.33}Co_{0.67}O_x$.

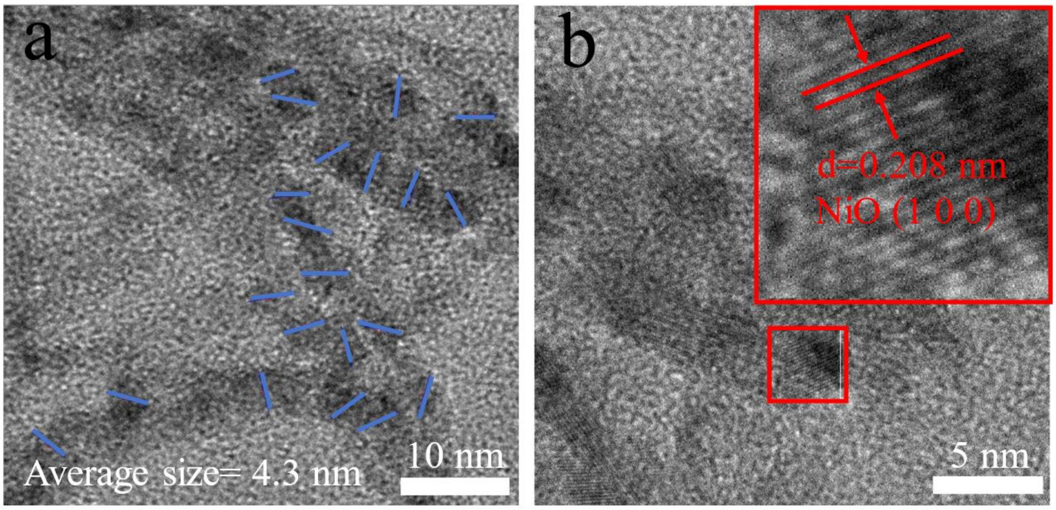

Fig. S4. a) TEM image and b) HRTEM image of NiO.

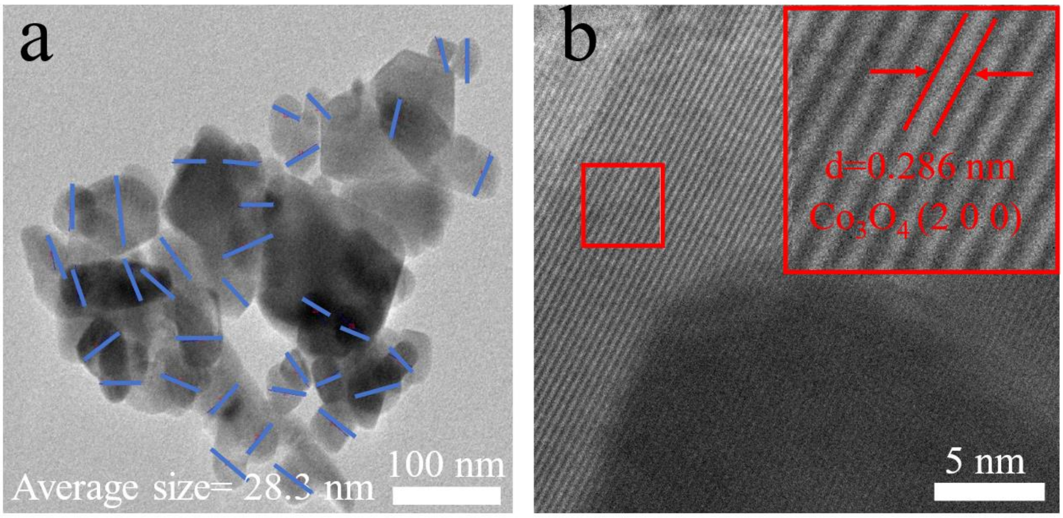

Fig. S5. a) TEM image and b) HRTEM image of Co_3O_4.

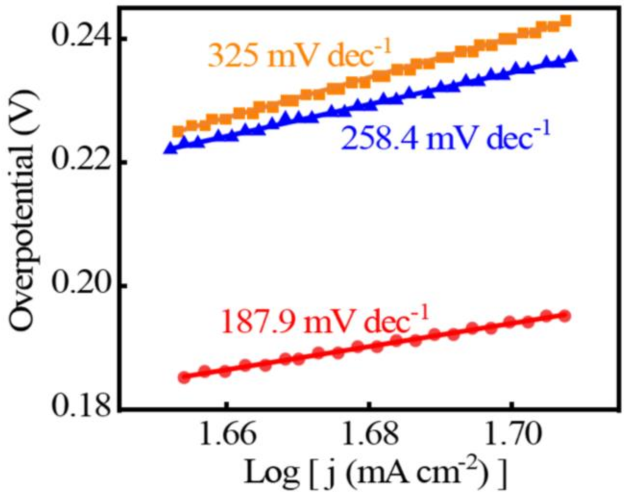

Fig. S6. Tafel plots measured of $Ni_{0.67}Co_{0.33}O_x$ (red), $Ni_{0.33}Co_{0.67}O_x$ (blue) and NiO (orange).

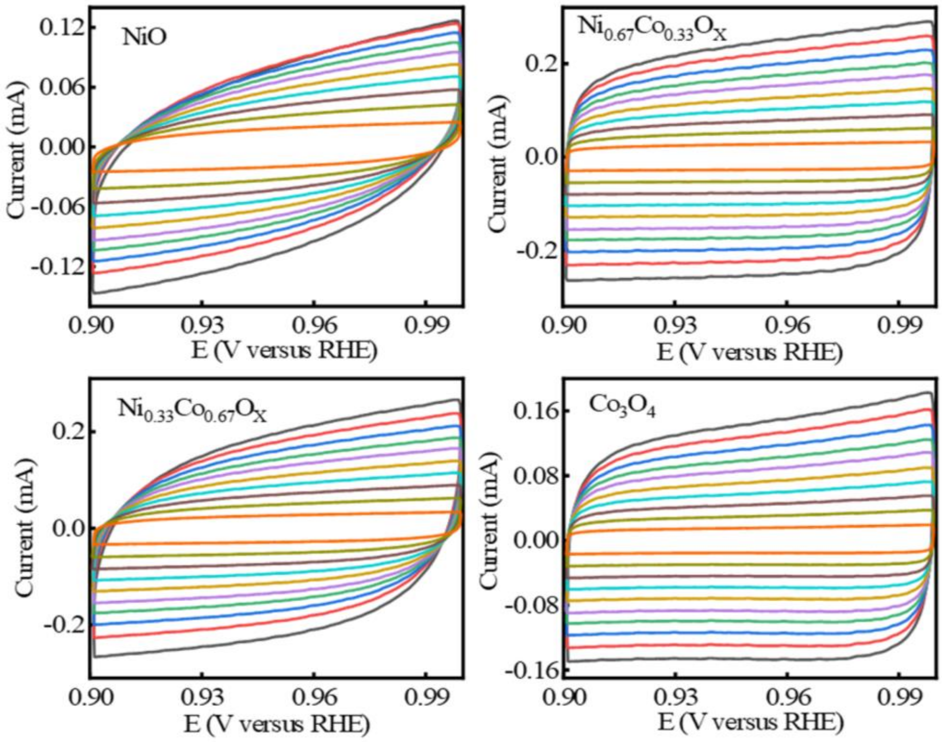

Fig. S7. CV curves in 1.0 M KOH in the non-faradaic potential range with a scan rate of 10–100 mV s^{-1}

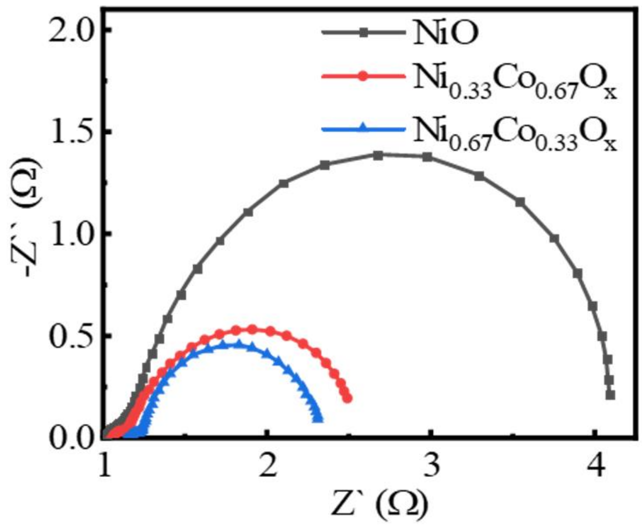

Fig. S8. The electrochemical impedance spectra of NiO, $Ni_{0.33}Co_{0.67}O_x$ and $Ni_{0.67}Co_{0.33}O_x$.

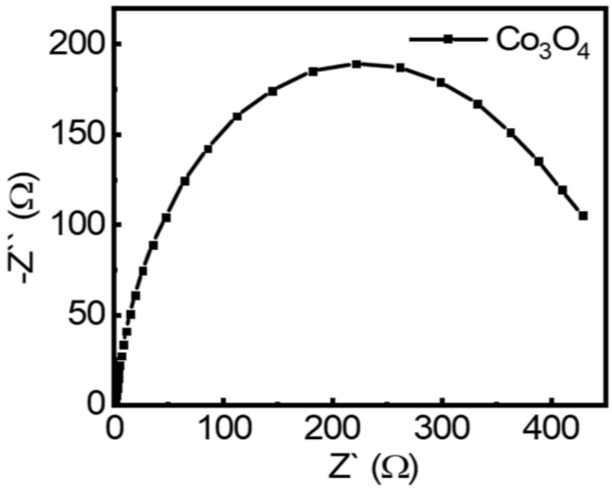

Fig. S9. The electrochemical impedance spectra of Co_3O_4.

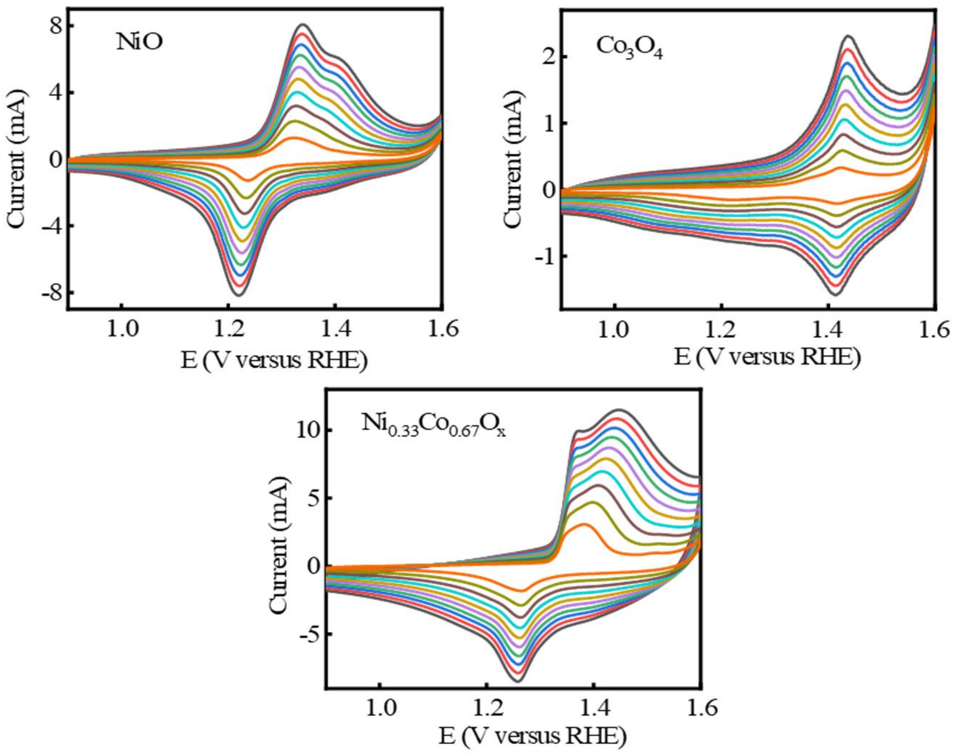

Fig. S10. CV curves in the potential range from 0.9 to 1.6 V with variable scan rate of 10-100 mV s^{-1}

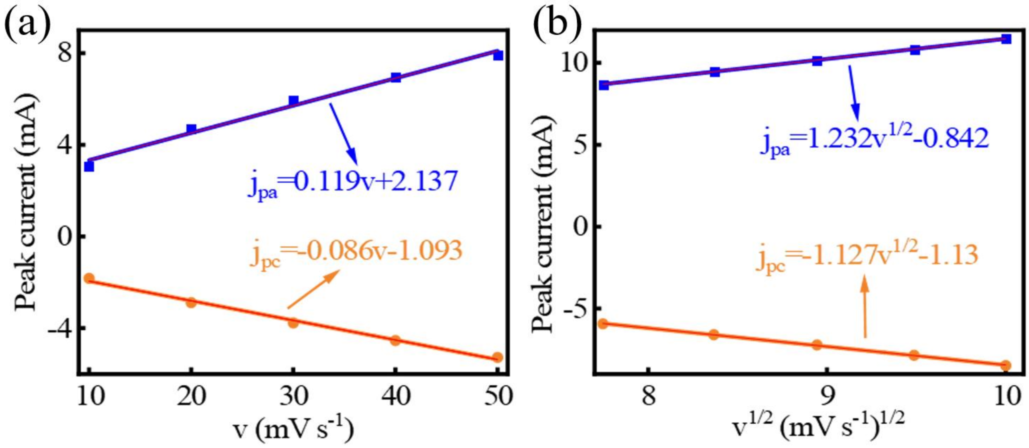

Fig. S11. a) Linear fit of peak current to scan rate for $Ni_{0.33}Co_{0.67}O_x$ electrode over a range of scan rates from 10 to 50 mV s^{-1}, b) the linear fitting of the peak current as a function of the square root of scan rate in the scan rate range from 60 to 100 mV s^{-1}.

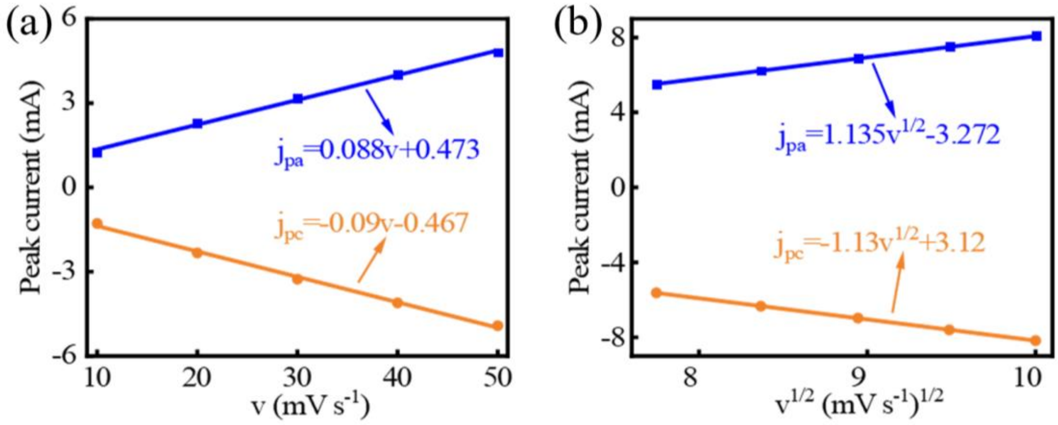

Fig. S12. a) Linear fit of peak current to scan rate for NiO electrode over a range of scan rates from 10 to 50 mV s^{-1}, b) the linear fitting of the peak current as a function of the square root of scan rate in the scan rate range from 60 to 100 mV s^{-1}.

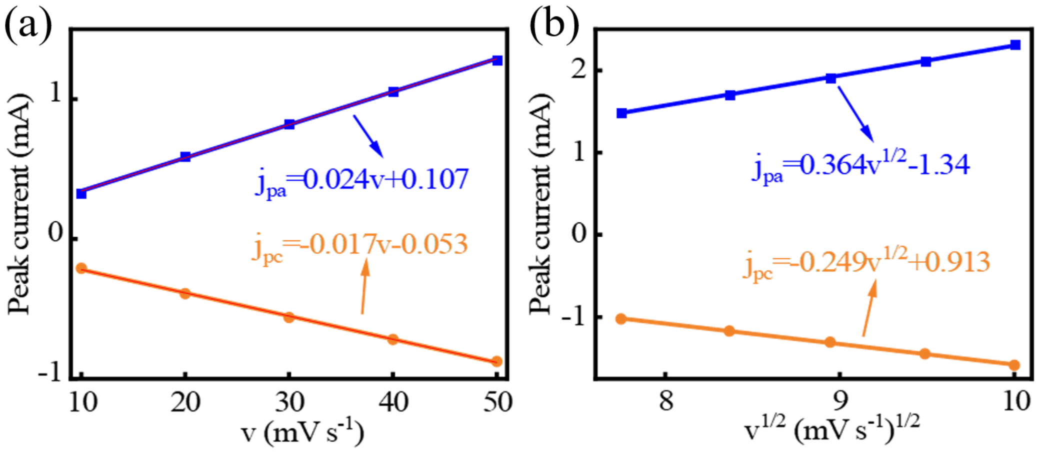

Fig. S13. a) Linear fit of peak current to scan rate for Co_3O_4 electrode over a range of scan rates from 10 to 50 mV s^{-1}, b) the linear fitting of the peak current as a function of the square root of scan rate in the scan rate range from 60 to 100 mV s^{-1}.

Table. S1. Product analysis for different voltage windows.

Potential (V)	1.4	1.5	1.6	1.7	1.8
molar concentration （mmol/L）	0.153	0.196	0.241	0.232	0.205
Dilution multiple	17	17	17	17	17
volume (L)	0.03	0.03	0.03	0.03	0.03
Coulomb (C)	42.82	50.38	55.33	74.2	67.26
Production (mmol)	0.078	0.099	0.123	0.118	0.105
FE (%)	70.33	76.53	85.74	71.54	60.11

Table. S2. The product analysis of $NiCoO_x$.

$NiCoO_x$	NiO	$Ni_{0.67}Co_{0.33}O_x$	$Ni_{0.33}Co_{0.67}O_4$	Co_3O_4
Dilution multiple	17	17	17	17
volume (L)	0.03	0.03	0.03	0.03
Coulomb (C)	744.96	1136.72	839.96	80.44
Production (mmol)	1.256	2.4	1.57	0.064
FE (%)	65.07	81.4	72.33	30.76

Table. S3. Comparison of the performance of the catalysts reported in this work with that of the alkaline ethanol oxidation catalysts already reported.

Electrocatalyst	Electrolyte	Onset potential	Peak density	stability	FE	references
Co_2NiO_4	1.0 M KOH + 0.5 M Ethanol	1.60 V (RHE)	87 mA cm^{-2}	~12%@2.78h	N/A	1
$NiCo_2O_4$/C	1.0 M KOH + 1.0 M Ethanol	1.60 V (RHE)	62 mA cm^{-2}	~67%@5h	N/A	2
$CoSeO_3$	1.0 M KOH + 1.0 M Ethanol	1.60 V (RHE)	71 mA cm^{-2}	83%@10h	~80%	3
B-Ni_2P/CoP/NF	1.0 M KOH + 1.0 M Ethanol	1.44 V (RHE)	20 mA cm^{-2}	N/A	N/A	4
NiFeOOH	1.0 M KOH + 1.0 M Ethanol	1.55 V (RHE)	92 mA cm^{-2}	64%@5h	77.4%	5
$Ni_{0.75}Co_{0.25}Se_2$	1.0 M KOH + 1.0 M Ethanol	1.50 V (RHE)	45 mA cm^{-2}	55%@27h	82.9%	6
Ni_3S_2 NWs	1.0 M KOH + 1.0 M Ethanol	1.50 V (RHE)	102 mA cm^{-2}	86%@16h	N/A	7
Ni_3S_2 NPs	1.0 M KOH + 1.0 M Ethanol	1.50 V (RHE)	83 mA cm^{-2}	84%@16h	N/A	7
$Ni(OH)_2$ NWs	1.0 M KOH + 1.0 M Ethanol	1.50 V (RHE)	35 mA cm^{-2}	76%@16h	N/A	7
$Ni_3Fe_{0.75}$	1.0 M KOH + 1.0 M Ethanol	1.50 V (RHE)	79 mA cm^{-2}	50%	80%	8
NiNPs-R	0.1 M NaOH + 0.2 M Ethanol	1.70 V (RHE)	21 mA cm^{-2}	54%@1.5h	62%	9
NiMoP/ERGO	0.1 M NaOH + 0.1 M Ethanol	1.80 V (RHE)	260 mA cm^{-2}	62.5%@1.2h	N/A	10
$Ni_{0.67}Co_{0.33}O_x$	1.0 M KOH + 1.0 M Ethanol	1.60 V (RHE)	126 mA cm^{-2}	95%@15h	85.74%	This work

Reference

1 M. Wang, D. Li, W. Jia, J. Zhao, J. Ma, D. Ma, T. Tang, T. Hu, J. Jia and H. Wu, *Electrochim Acta*, 2022, **411**, 140048.

2 L. Jia, Y. Wang, D. Duan, X. Zhou, S. Liu and Q. Wei, *J Alloys Compd*, 2024, **984**, 173974.

3 S. E. Michaud, M. M. Barber, K. E. Rivera Cruz and C. C. L. McCrory, *ACS Catal*, 2023, **13**, 515–529.

4 Z. Xu, Y. Ye, Z. Chen, Z. Chen, J. Chen, F. Xie, Y. Jin, N. Wang and H. Meng, *Chemical Communications*, 2023, **59**, 8392–8395.

5 J. Xu, B. X. Wang, D. Lyu, T. Wang and Z. Wang, *Int J Hydrogen Energy*, 2023, **48**, 10724–10736.

6 J. Li, X. Wang, C. Xing, L. Li, S. Mu, X. Han, R. He, Z. Liang, P. Martinez, Y. Yi, Q. Wu, H. Pan, J. Arbiol, C. Cui, Y. Zhang and A. Cabot, *Chemical Engineering Journal*, 2022, **440**, 135817.

7 Y. Zhang, W. Zhu, J. Fang, Z. Xu, Y. Xue, D. Liu, R. Sui, Q. Lv, X. Liu, Y. Wang, W. Chen and Z. Zhuang, *Nano Res*, 2022, **15**, 2987–2993.

8 J. Li, L. Li, X. Ma, J. Wang, J. Zhao, Y. Zhang, R. He, Y. Yang, A. Cabot and Y. Zhu, *Nano Res*, 2024, **17**, 2328–2336.

9 S. Chemchoub, L. Oularbi, A. El Attar, S. A. Younssi, F. Bentiss, C. Jama and M. El Rhazi, *Mater Chem Phys*, 2020, **250**, 123009.

10 K. Rahmani and B. Habibi, *Int J Hydrogen Energy*, 2020, **45**, 27263–27278.